Journal of Nuclear Materials 389 (2009) 420–426

Contents lists available at ScienceDirect

Journal of Nuclear Materials

journal homepage: www.elsevier.com/locate/jnucmat

Effect of thermo-mechanical processing on microstructure and creep properties of the foils of alloy 617

S.K. Sharma [a], C. Jang [b], K.J. Kang [a,*]

[a] Department of Mechanical Engineering, Chonnam National University, 300-Yongbong Dong, Buk-gu, Gwangju 500 757, Republic of Korea
[b] Department of Nuclear and Quantum Engineering, Korea Advanced Institute of Science and Technology (KAIST), 373-1 Guseong-Dong, Yuseong-gu, Daejeon 305 701, Republic of Korea

ARTICLE INFO

Article history:
Received 31 August 2008
Accepted 14 February 2009

PACS:
81.40−z
81.40.Ef
61.72.Mm
62.40.Hg
81.65.Mg

ABSTRACT

The effect of rolling and annealing on the microstructure and high temperature creep properties of alloy 617 were investigated. Two types of foil specimens with different thickness reductions were prepared by thermo-mechanical processing. Recrystallization and grain growth were readily observed at specimens annealed at 950 and 1100 °C. The uniform coarse grains increase resistance against creep deformation. The grain size effect in creep deformation was dominant up to 900 °C, while dynamic recrystallization effect became dominant at 1000 °C. Dynamic recrystallization was observed in all the creep deformed foils, even though some specimens had already been (statically) recrystallized during annealing. Steady state creep rates decreased with increasing annealing temperature in the less rolled foils. The apparent activation energy Q_{app} for the creep deformation increased from 271 to 361 kJ/mol as the annealing temperature increased from 950 to 1100 °C.

1. Introduction

A contemporary concept for the development of generation-IV (GEN-IV) reactors is considered for producing electricity and hydrogen economically. Very high temperature gas-cooled reactor (VHTR) is the most promising reactor type among the GEN-IV reactors. The predicted service temperature of a VHTR can reach up to 850 °C or higher. Also, a coolant gas pressure of up to 8 MPa is being considered. Therefore, the structural materials of the VHTR must survive in the harsh conditions for the lifetime of the reactor up to 60 years. Ni-base alloys, especially the solution hardening alloys, are candidate materials for VHTR due to their excellent material properties; namely, oxidation resistance, creep strength, and phase stability at high temperatures. Alloy 617 has been selected as a potential candidate for use in the construction of the piping and heat exchangers of the VHTR [1,2]. Alloy 617 is an austenitic solid-solution strengthened Ni-base alloy which contains chromium (Cr), cobalt (Co), molybdenum (Mo), Carbon (C) and aluminum (Al). Al and Cr contents protect the alloy from oxidation reaction at high temperatures. Mo and Co provide solid-solution strengthening, and C contributes strengthening by $M_{23}C_6$ carbide precipitation [3–8]. Alloy 617 is normally used in the annealed condition, which provides a coarse grain structure to realize the best creep rupture strength [9,10].

Nickel-base alloys are subject to degradation due to creep when they are exposed to the VHTR operating environment for a prolonged period. Therefore, the creep properties of candidate alloys should be well understood and thoroughly characterized before the alloys are used in the design and construction of components of a VHTR. The creep rupture lives are known to be strongly dependent on the alloy's microstructure as well as the test temperatures and the applied stresses [10,11].

The techniques for measuring creep properties have been standardized for round bar specimens of metals. However, there is no standard available for testing with miniaturized specimens, which are necessary to reduce cost and volume of material testing equipment. Lucas [12] and Jung et al. [13] have reviewed small specimen techniques used to evaluate irradiation embrittlement of materials and recommend some of them. It is the opinion of the authors that international efforts should be concentrated on further development of testing techniques for miniaturized samples, and a detailed correlation between miniature and bulk behavior. Economical creep testing systems of high temperature alloys have been developed by Volki et al. [14] and Kang and co-workers [15–17]. Joule heating was chosen for easy access to the sample, quickly attainable heating and cooling rates, and simplicity in design and operation. Volki et al. [14] performed creep tests for the foils of pure Pt and Pt-based alloys, and strain was measured with a video extensometer by means of the software 'super-creep'. Kang and co-workers [15] measured the creep strain by a laser interferometer.

* Corresponding author. Tel.: +82 62 530 1668; fax: +82 62 530 1689.
E-mail address: kjkang@chonnam.ac.kr (K.J. Kang).

0022-3115/$ - see front matter © 2009 Elsevier B.V. All rights reserved.
doi:10.1016/j.jnucmat.2009.02.029

For miniaturizing test systems, the foil specimen was a fundamental requirement. Thermo-mechanical processing (TMP) is a method to prepare foil specimens. TMP is a combination of cold rolling and recrystallization. During the cold rolling of a metal, some of the energy involved in the deformation is stored as dislocations and point defects. Upon annealing, a large number of point defects are reduced, and dislocations rearrange themselves into lower energy configurations. The grain size of the cold rolled and annealed alloys is affected by chemical composition, reduction in thickness, annealing temperature, and time [18–24].

The characterizations and measurements of microstructures are of great importance to material scientists because grain size strongly affects mechanical properties, physical properties, surface properties, and phase transformations [25]. The ability to control the grain size/boundary in materials is critical for a wide range of applications; e.g., process control and optimization. Creep properties also depended markedly on grain size as well as applied stress, and temperature under all deformation conditions [26]. Muto et al. [27] have observed that the creep strain rate increases with decreasing grain size for the Cu-based alloy. Youssef et al. [28] observed a similar result for Al-based alloys. Consequently, it was suggested that the mechanism of creep deformation for the tested alloy is related to grain boundary sliding and dynamic recrystallization.

The intent of this research is to investigate the rolling and annealing effect on microstructure, and associated hardness, creep properties of the foils of alloy 617. The microstructures of thermo-mechanically processed specimens for various sizes and shapes of grains were examined under an optical microscope. Hardness tests were taken for all the as-rolled and rolled-annealed foils. Creep tests were performed to evaluate the influence of grain sizes, temperatures, and applied stresses on the creep rupture life, rupture strain, steady state creep rate, and associated microstructure transformation such as dynamic recrystallization. The steady state creep rate $\dot{\varepsilon}_{ss}$ and the apparent activation energy Q_{app} for creep deformation were calculated from the experimental results.

2. Experimental protocol

2.1. Materials and preparation

Commercially available alloy 617 was used for the experiments. The foils were prepared under thermo-mechanical processing (TMP). Namely, a thick plate was wire-cut into strips of thickness 0.5–1.0 mm, then, the strips were annealed in a vacuum (as being enclosed in a vacuum sealed quartz tube). And the strips were rolled into foils of thickness ~100 μm. Some of them were annealed again at 950 or 1100 °C in vacuum for 17 h. Table 1 lists the abbreviations of the specimens according to the six different preparation processes. Surface oxides were then removed by surface-polishing with 1000, 1200, and 1500 grit SiC papers. Polishing was also performed with a paste of 1 μm diamond suspension. After each preparation step, the specimens were thoroughly cleaned ultrasonically with acetone and dried by blowing with pure compressed nitrogen gas. The dimensions and weight were measured before and after each experiment within accuracies of ±10 μm and ±10 μg, respectively.

Table 1
Abbreviations of various foil specimens of alloy 617 used for the experiments.

	88% Thickness reduction	64% Thickness reduction
Rolled	R-1	R-2
Rolled-annealed at 950 °C for 17 h	R-1A:950	R-2A:950
Rolled-annealed at 1100 °C for 17 h	R-1A:1100	R-2A:1100

2.2. Micro-creep test system and measurement

A specially designed test machine was used to measure creep response of the foil specimens. Electricity passed through the specimen to obtain high temperature. The oxide thickness and strain developed on the surface were monitored in situ. The detailed operation mechanism and specifications are given in Refs. [15,16]. Next, a fixed load P was applied, and the creep displacement was recorded continuously. After the creep fracture, the specimen was removed from the test system. And the specimen was mounted with resin and polished up to a 1 μm diamond suspension. After polishing, the specimen was etched at room temperature in HCl-15 ml/

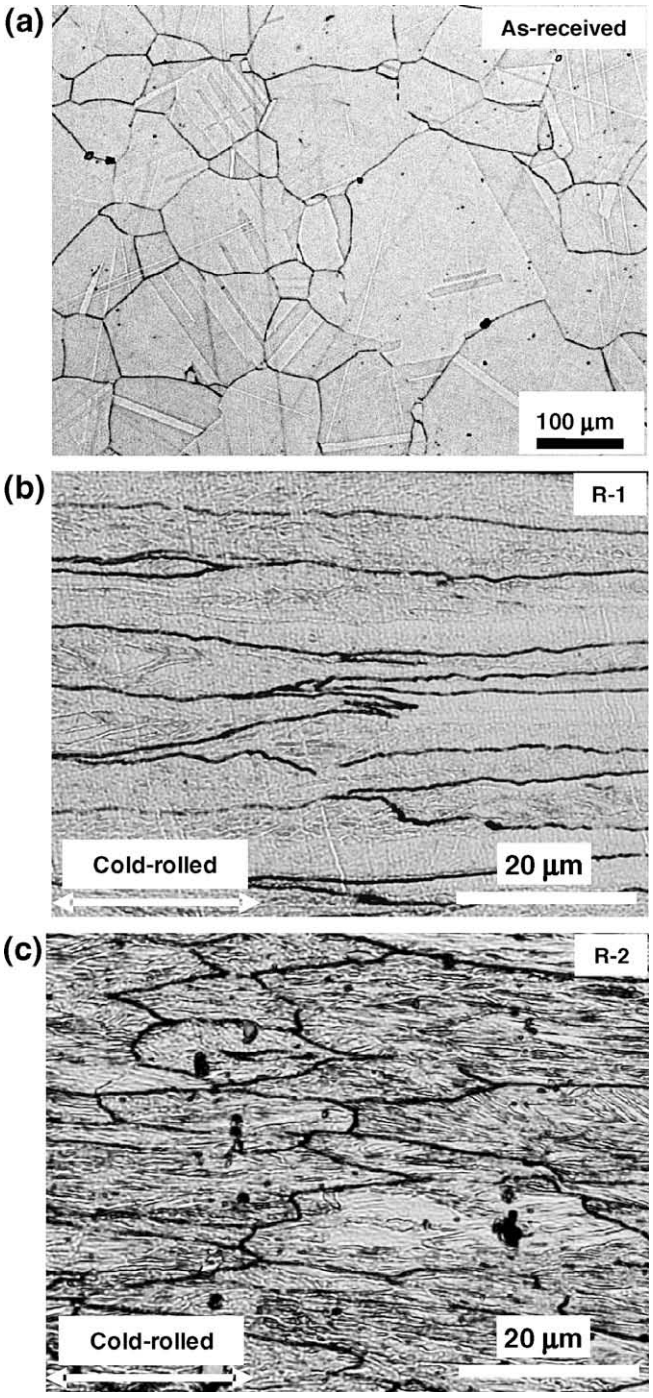

Fig. 1. Microstructures of alloy 617 (a) as-received, (b) R-1 (88% thickness reduction), and (c) R-2 (64% thickness reduction).

HNO_3-5 ml solution for 60–90 s. The specimen microstructure near the fracture was then observed under an optical microscope.

3. Results and discussion

3.1. Effect of rolling and annealing on microstructure and recrystallization

The microstructures of as-received and heavily cold rolled foils of alloy 617 with a thickness reduction of 88% and 64%, named R-1 and R-2, are shown in Fig. 1(a–c), respectively. The black grain boundary in Fig. 1(a) represents the carbide-rich grain boundaries which were elongated along rolling direction in the rolled specimens, R-1 and R-2. The grains in R-1 were more lengthened along the rolling direction than those in R-2 because of the higher thickness reduction. The different thickness reductions resulted in different microstructures in the rolled-annealed specimens regardless of the annealing temperature. Fig. 2(a) and (b) shows the microstructures after R-1 and R-2 were vacuum-annealed at 950 °C for 17 h which are named R-1A:950 and R-2A:950, respectively. The grain sizes in both R-1A:950 and R-2A:950 foils ranged from 2 to 10 μm. While chains of the carbide island were observed in R-2A:950, no carbide was observed in R-1A:950; the chains might be shattered due to the higher thickness reduction in rolling. Fig. 2(c) and (d) shows the microstructures after R-1 and R-2 were vacuum-annealed at 1100 °C for 17 h which are named R-1A:1100 and R-2A:1100, respectively. The grain sizes in both annealed foils, R-1A:1100 and R-2A:1100 were observed to range from 5 to 30 μm. The higher annealing temperature resulted in the larger grains. In comparison with the microstructures of the rolled specimens shown in Fig. 1(b) and (c), those of the rolled and annealed specimens reveal severe recrystallization. Similar recrystallization had been observed in the identical material, alloy 617, by Mino et al. [29]. The extent of recovery was determined by hardness measurement tests after each treatment of alloy 617 foils, and compared with as-received commercially available alloy 617.

3.2. Vickers hardness of treated foils of alloy 617

The variation of Vickers hardness and grain size of treated foils, i.e., as-received, rolled by 88% (R-1), rolled by 64% (R-2), and annealed foils, are shown in Fig. 3. The grain sizes of the samples were influenced by rolling and annealing, and those were differentiated under a hardness test. The grain size in rolled-annealed foils was observed lower than those of as-received foils and rolled foils. The hardness was found to be the highest in R-1 (cold rolled – 88%), and the lowest in R-2A:1100 (rolled-annealed at 1100 °C for 17 h). The hardnesses of the foils annealed at 1100 °C, R-1A:1100 and R-2A:1100, were similar to that of the as-received one. However, the hardness of rolled-annealed foils at a lower annealing temperature of 950 °C was higher than that of rolled-annealed foils at a higher temperature of 1100 °C.

3.3. Rolling and annealing effects on creep properties of foils

The creep tests were carried out at 900 °C in an air environment with an applied stress of 35 MPa, and the results showed the substantial effect of rolling and annealing. The creep curves for the foils of alloy 617 such as R-1, R-2, R-1A:950, R-2A:950, and R-2A:1100 are shown in Fig. 4. For the as-rolled specimens, the creep rate of R-2 was found to be lower than that of R-1, and accordingly the life of R-2 was longer than that of R-1. After annealed at 950 °C, however, the creep rate of R-2A:950 was higher than that of R-1A:950, and accordingly the creep life of R-2A:950 was shorter in than R-1A:950. The creep life of R-2A:1100 was the longest. From these result, it is seen that the annealing at the higher temperature reinforced the creep strength of the rolled specimens.

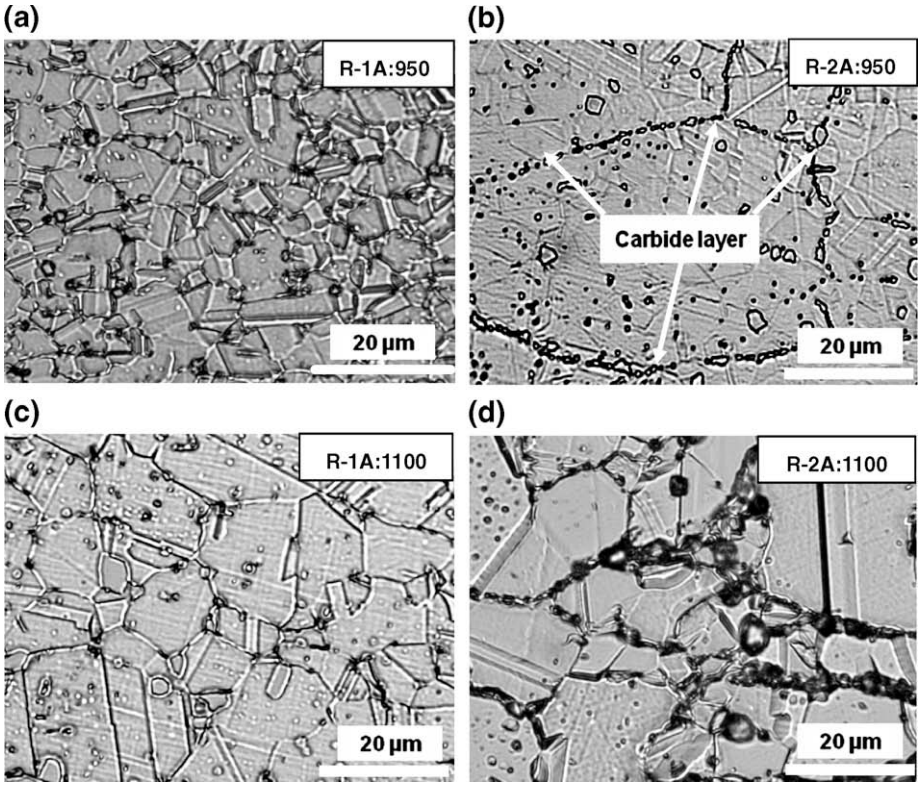

Fig. 2. Microstructures of rolled-annealed foils of alloy 617 at 950 °C, (a) R-1A:950, (b) R-2A:950 and rolled-annealed at 1100 °C, (c) R-1A:1100, and (d) R-2A:1100.

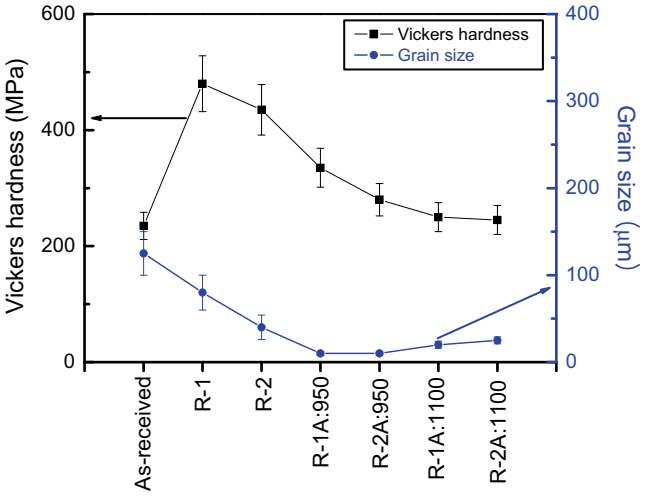

Fig. 3. Variation of Vickers hardness and grain size versus the foils of alloy 617 such as as-received, R-1, R-2, R-1A:950, R-2A:950, R-1A:1100, and R-2A:1100.

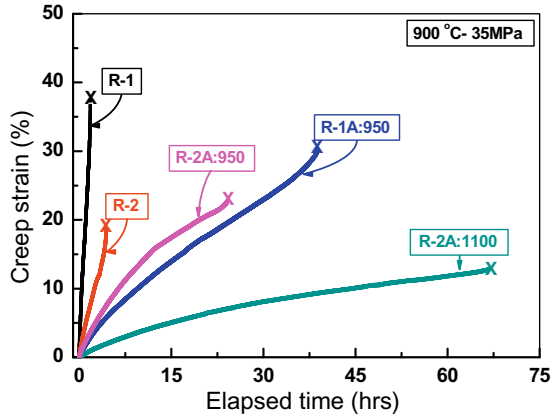

Fig. 4. Curves of creep strain versus elapsed time for alloy 617 foils at typical temperature of 900 °C of applied stress of 35 MPa in air.

Considering the creep properties and hardness measured for the rolled-annealed foils, further investigations were focused on the two kinds of specimens, i.e., R-1A:950 and R-2A:1100. First, creep tests were performed under an applied stress of 48 MPa at three different temperatures, i.e., 800, 900, and 1000 °C. Fig. 5(a–c) shows the creep curves of the rolled-annealed foils, respectively. As shown in Fig. 5(a), the creep rupture life was much longer for the specimen R-2A:1100 prepared with the lower thickness reduction and higher annealing temperature. That is, the creep rupture life increased from ~60 h of R-1A:950 to more than 325 h of R-2A:1100. Similar creep behavior was observed at 900 °C. However, at 1000 °C, as shown in Fig. 5(c), R-1A:950 withstood an exceptionally large strain before fracture, and its creep life was longer than that of R-2A:1100, even though the strain rates were still higher in R-1A:950. This strange behavior seems to be attributed to material softening due to more active dynamic recrystallization during the deformation without void nucleation.

Overall creep strength of the foil specimens in this work, scaled by life, were much lower than those measured for ordinary round bar specimens [17,29]. There are two possible sources for the discrepancy. First, all the specimens in this work were heavily rolled in preparation, which induced dynamic recrystallization in their microstructure during deformation under creep load even after annealed. The evidence of dynamic recrystallization was observed in the microstructure of the creep-tested specimen which will be

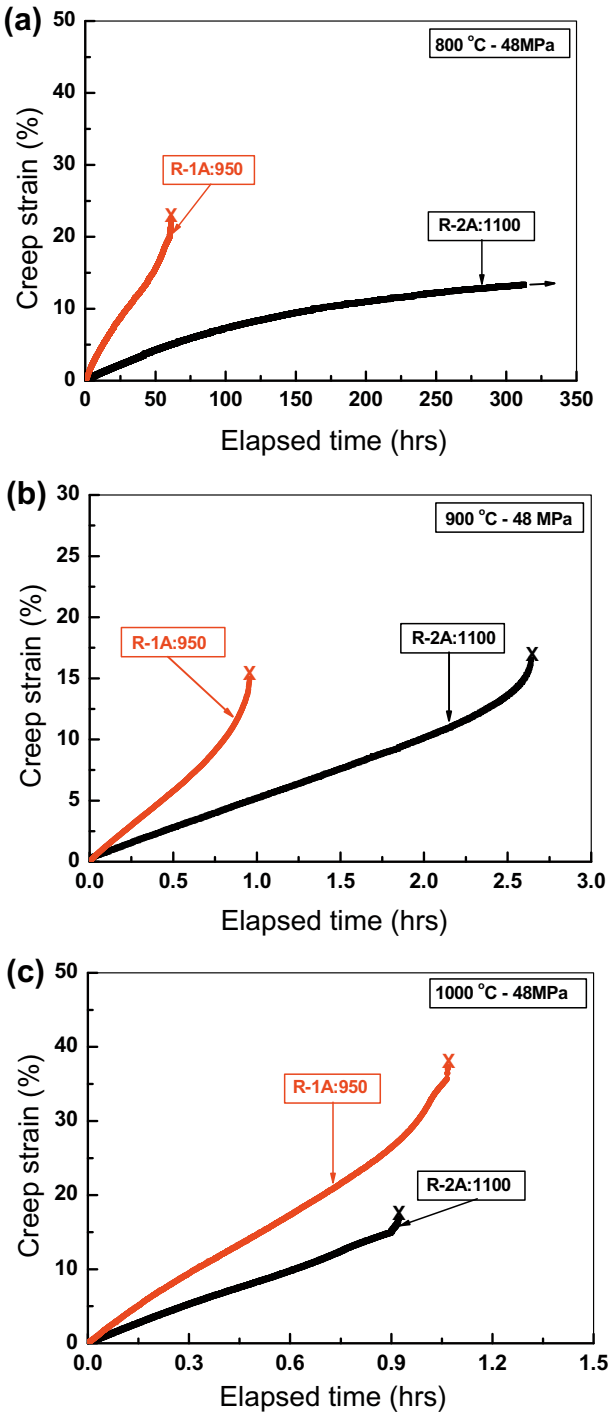

Fig. 5. Curves of creep strain versus elapsed time for alloy 617 foils of applied stress of 48 MPa in air at (a) 800 °C, (b) 900 °C, and (c) 1000 °C.

discussed in the Section 3.5. Similar softening due to the dynamic recrystallization has been reported for Type 347 stainless steel [30], alloy 617 [31] and Hastelloy XR [32]. Secondly, the thickness of the specimens in this work was only 100 μm, whereas the specimens of Mino et al. [29] had the diameter of 3 or 6 mm. Accordingly, size effect might result in the difference in their creep strength.

3.4. Steady state creep rates and activation energy

Fig. 6 shows the creep rates of the foils versus foil specimens of alloy 617 such as R-1, R-2, R-1A:950, and R-2A:1100. The steady

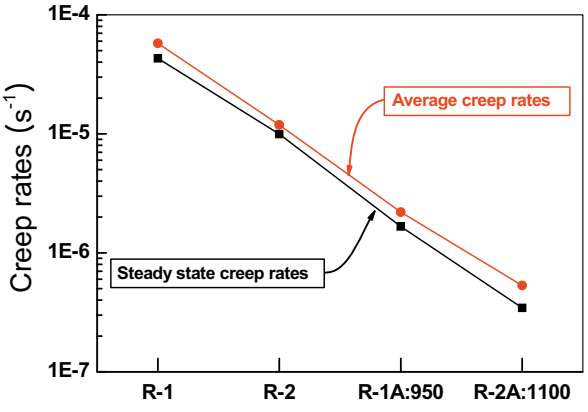

Fig. 6. Variation of creep rates versus treated foils of alloy 617.

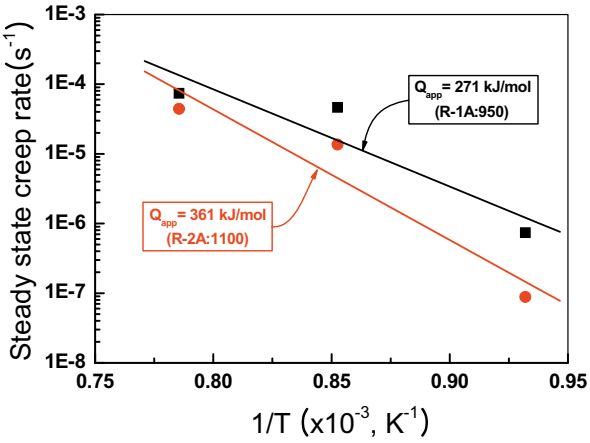

Fig. 7. Variation of steady state creep rates versus inverse temperature of applied stress of 48 MPa.

state creep rates and average creep rates decreased from as-rolled to rolled-annealed foils. The steady state creep rates and average creep rates were found to be lower in R-2 than in R-1 because of lower thickness reduction. For the rolled-annealed foil specimens, the creep rates were even lower. The creep rates were the lowest for R-2A:1100 with the lower thickness reduction and higher annealing temperature.

The steady state creep rates, $\dot{\varepsilon}_{ss}$, in crystalline materials involves a thermally activated process [33–35] described by $\dot{\varepsilon}_{ss} = A\sigma^n \exp(-Q_{app}/RT)$, where σ is the applied stress, n is the stress exponent, Q_{app} is the apparent activation energy for the creep mechanism, A is a constant, R is the universal gas constant $\sim$8.368 JK^{-1} mol^{-1}, and T is the absolute temperature. The apparent activation energy, Q_{app}, was calculated from the equation: $\log \dot{\varepsilon}_{ss} \propto 0.217 Q_{app}(1/T)$. Fig. 7 shows the plot of steady state creep rates ($\log \dot{\varepsilon}_{ss}$) on log scale versus inverse temperature ($1/T$) on linear scale. The straight lines in the figure show the linear fit of the experimental data. The value of $0.217Q_{app}$ was equivalent to the slope of the linear fit. The calculated values of Q_{app} are inserted in the figure for the foils R-1A:950 and R-2A:1100. The Q_{app} for creep deformation in air environment increased from 271 to 361 kJ/mol as the annealing temperature increased from 950 to 1100 °C and thickness reduction decreased from 88% to 64%. The value Q_{app} = 271 kJ/mol is very close to 270 kJ/mol, observed for the bulk specimens in the He + O_2 environment [10]. The increased activation energy is attributed to the enhancement in resistance for creep deformation.

3.5. Microstructure of creep-tested foils

The microstructures of the specimens, i.e., R-1, R-2, R-1A:950, and R-2A:1100 which were creep-tested at 900 °C under an applied stress of 35 MPa were shown in Fig. 8(a–d), respectively. The photos were taken near the fractured region along the lateral direction. Compared with the photos taken before the creep tests, shown in Figs. 1(b) and (c), 2(a) and (d), respectively, all the microstructures reveal recrystallization occurred during creep deformation, that is,

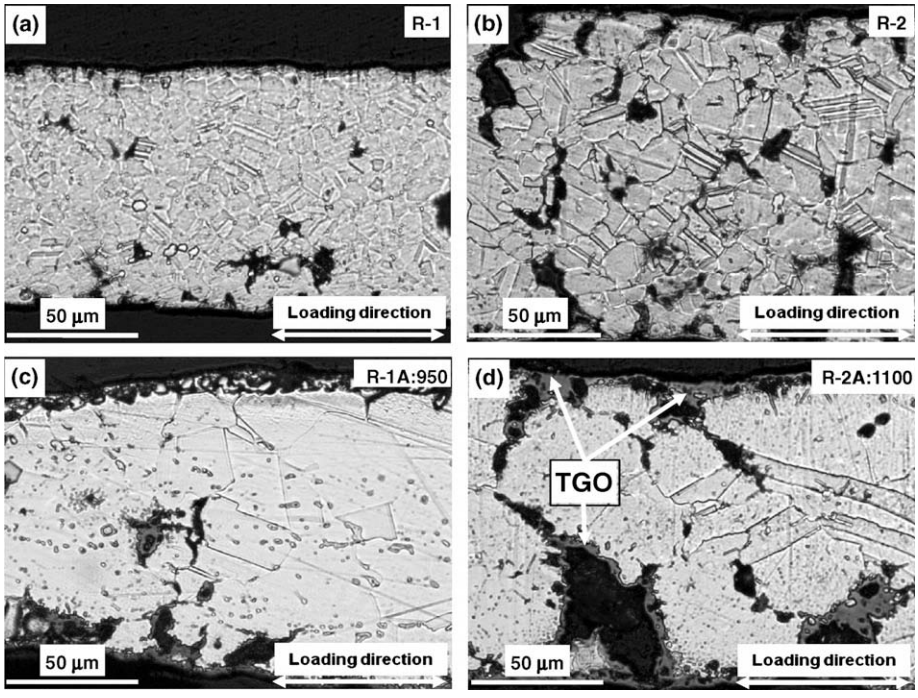

Fig. 8. Microstructures of creep-tested foils of alloy 617 along lateral exterior near fracture region (a) R-1; (b) R-2; (c) R-1A:950; and (d) R-2A:1100.

dynamic recrystallization (DRX). DRX is an effective metallurgical process for grain refinement during hot deformation. DRX is a typical softening mechanism during hot deformation caused by the generation and migration of high angle boundaries inside the sub-grains [36–38]. Voids were also observed in all the specimens along the grain boundaries. The voids were lengthened perpendicular to the loading direction. Thermally grown oxides (TGOs), that is, chromia (Cr_2O_3) was observed to most often in R-2A:1100 on the surface and along the void boundaries because of the longest elapsed time. The thicker TGO indicates more vacancy diffusion. The cavity growth process at grain boundaries at elevated temperature has long been suggested to involve vacancy diffusion.

The microstructures of the two rolled-annealed specimens, i.e., R-1A:950 and R-2A:1100 which were creep-tested at 900 °C under an applied stress of 48 MPa were shown in Fig. 9(a) and (b), respectively. The voids were observed near the fracture surface in R-1A:950 along the grain boundaries, while in R-2A:1100, no voids and more active DRX were observed. Fig. 9(c) and (d) shows cracks propagated from the surface to interior along the grain boundaries. The crack propagation was found more often in R-2A:1100. Fig. 9(e) and (f) shows the DRX at the interior near the fracture region. The grain sizes were found to be approximately similar in both specimens.

4. Conclusion

The effect of rolling and annealing on the microstructure and high temperature creep properties of alloy 617 were investigated with six different kinds of foil specimens, i.e., R-1, R-2, R-1A:950, R-2A:950, R-1A:1100, and R-2A:1100.

(i) The grain sizes in rolled-annealed foils were lower than those of as-received foils and rolled foils, because of recrystallization occurred in the annealing. The annealing also reduced the hardness, which was the lowest in R-2A:1100.

(ii) However, the annealing induced the higher resistance against creep deformation regardless of the applied stress level. Between the two rolled-annealed foils, R-1A:950 and R-2A:1100, the latter showed the higher resistance against creep deformation at all the test temperatures, although the former showed exceptionally high elongation at 1000 °C.

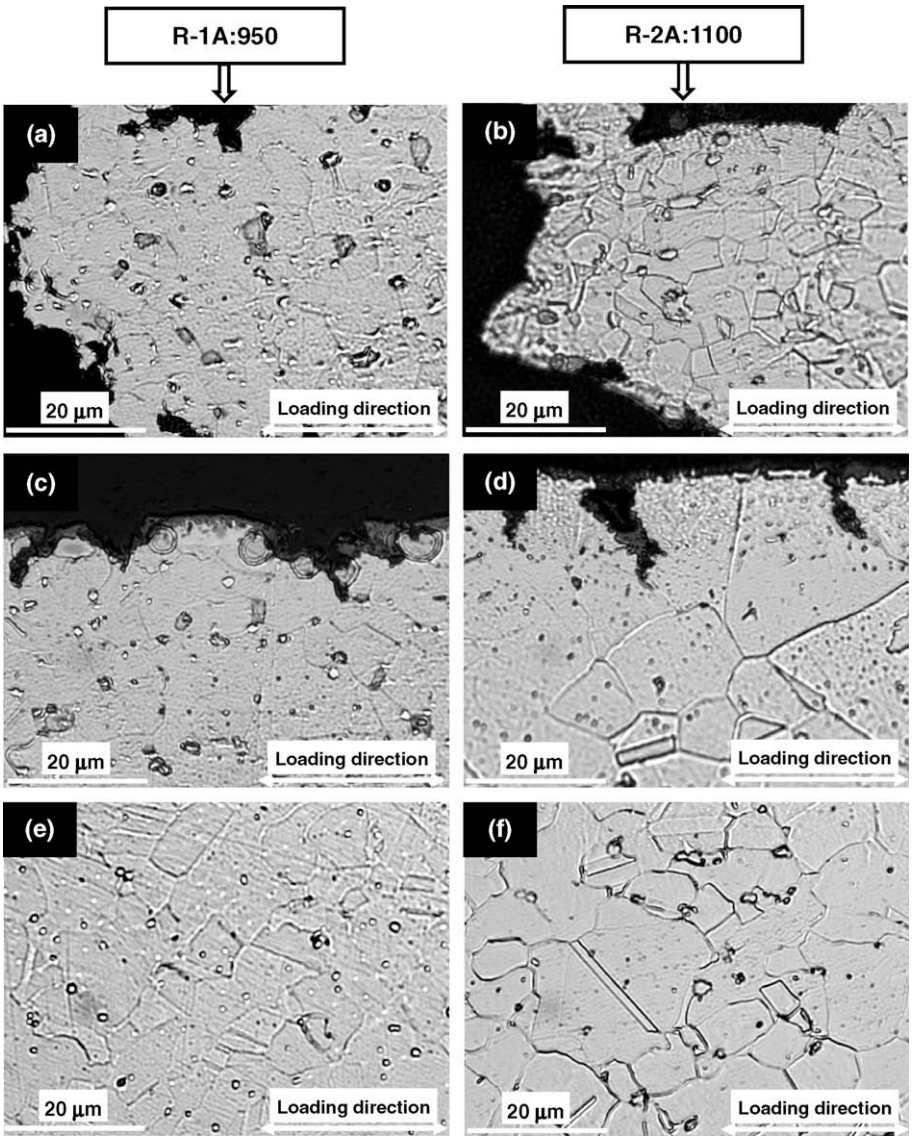

Fig. 9. Microstructures of creep-tested foils of alloy 617 at 900 °C of applied stress of 48 MPa for R-1A:950 and R-2A:1100, (a) and (b) for the fracture surface, (c) and (d) for initiation of the fracture, (e) and (f) for interior near the fracture region.

(iii) All the foils showed dynamic recrystallization during creep deformation because of high thickness reduction experienced by rolling in the specimen preparation. The dynamic recrystallization was one of main sources of the low creep strength compared with those found from literatures. Accordingly, the less rolled and more annealed foils such as R-2A:1100, which showed the least dynamic recrystallization, resulted in the highest creep strength.

Acknowledgements

This work was supported by the Basic Atomic Energy Research Institute (BAERI: 2007-01634), which is a part of the Nuclear R&D Programs of the Ministry of Education, Science & Technology (MEST), and one of the authors, S.K. Sharma, was financially supported by the second phase BK-21 Program, Korea. The authors would like to thank Dr J.W. Choi, POSCO, Korea for rolling the foils.

References

[1] T. Angeliu, J. Ward, J. Witter, Assessing the Effects of Radiation Damage on Ni-Base Alloys for the Prometheus Space Reactor System, LM-06K033, P.O. Box 1072, Schnecetady, New York, USA, April 2006.
[2] R.N. Wright, Summary of Studies of Aging and Environmental Effects on Inconel 617 and Haynes 230, INL/EXT-06-11750, September 2006.
[3] F.M. Olbersleben, N. Kasik, B. Ilschner, F.R. Aria, Metall. Mater. Trans. A 30 (1999) 981.
[4] C. Jang, D. Lee, D. Kim, Int. J. Press. Vess. Pip. 85 (2008) 368.
[5] A. Kewther, B.S. Yilbas, M.S.J. Hashmi, J. Mater. Eng. Perform. 10 (2001) 108.
[6] M.A. Kewther, B.S. Yilbas, M.S.J. Hashmi, Indust. Lub. Tribol. 53 (2001) 112.
[7] M.K. Ali, M.S.J. Hashmi, B.S. Yilbas, J. Mater. Proc. Tech. 118 (2001) 45.
[8] D. Allen, J.P. Keustermans, S. Gijbels, V. Bicego, Mater. High Temp. 21 (2004) 55.
[9] L. Tan, K. Sridharan, T.R. Allen, J. Nucl. Mater. 371 (2007) 171.
[10] P.S. Shankar, K. Natesan, J. Nucl. Mater. 366 (2007) 28.
[11] M. Tamura, H. Esaka, K. Shinozuka, ISIJ Int. 39 (1999) 380.
[12] G.E. Lucas, Metall. Trans. A 21 (1990) 1105.
[13] P. Jung, A. Hishinuma, G.E. Lucas, H. Ullmaier, J. Nucl. Mater. 232 (1996) 186.
[14] R. Volki, D. Freund, B. Fischer, J. Test. Eval. 31 (2003) 35.
[15] S.S. Lee, S.K. Sun, K.J. Kang, Oxid. Met. 63 (2005) 73.
[16] K.J. Kang, C. Mercer, Mater. Sci. Eng. A 478 (2008) 154.
[17] S.K. Sharma, G.D. Ko, F.X. Li, K.J. Kang, J. Nucl. Mater. 378 (2008) 144.
[18] B. Bhattacharya, R.K. Ray, Metall. Mater. Trans. A 35 (2004) 71.
[19] J. Chen, T. Muroga, T. Nagasaka, Y. Xu, S. Qiu, J. Nucl. Mater. 322 (2003) 73.
[20] S.H. Hong, D.N. Lee, Mater. Sci. Eng. A 357 (2003) 75.
[21] H. Borodianska, M. Demura, K. Kishida, T. Hirano, Intermetallics 10 (2002) 255.
[22] I. Baker, Intermetallics 8 (2000) 1183.
[23] F. Scholz, J.H. Driver, E. Woldt, Scr. Mater. 40 (1999) 949.
[24] Y. Lin, X. Wu, J. Ke, R.W. Chan, Phys. Stat. Sol. (a) 167 (1998) 29.
[25] F.J. Humphreys, J. Mater. Sci. 36 (2001) 3833.
[26] J.P. Poirier, Creep of Crystals: High Temperature Deformation Processes in Metals, Ceramics and Minerals, Cambridge University, Cambridge, 1985.
[27] A. Muto, S. Goto, M. Tagami, S. Aso, J. Mater. Sci. Soc. Jpn. 35 (1998) 251.
[28] S.B. Youssef, M.H.N. Beshai, A. Fawzy, M. Sobhy, G. Saad, Cryst. Res. Tech. 30 (1995) 1017.
[29] K. Mino, A. Ohtomo, Y. Saiga, Tetsu To Hagane 63 (1977) 2372.
[30] M.J. Grant, A.G. Bucklin, W. Rowland, Trans. ASM 48 (1956) 446.
[31] K. Mino, A. Ohtomo, Y. Saiga, Tetsu To Hagane 63 (1977) 2372.
[32] Y. Kurata, S. Hamada, H. Nakajima, in: Proceedings of the 10th International Conference on the Strength of Materials (ICSMA-10), 21–26 August 1994, Sendai, Japan, p. 627.
[33] J.S. Huo, J.T. Gou, L.J. Zhou, X.Z. Qin, G.S. Li, J. Mater. Eng. Perform. 16 (2007) 55.
[34] T.C. Totemeier, T.M. Lillo, Metall. Mater. Trans. A 36 (2005) 785.
[35] N.E. Dowling, Mechanical Behavior of Materials, 2nd Ed., Prentice Hall, New Jersey, USA, 1999.
[36] E. Brunger, X. Wang, G. Gottstein, Scr. Mater. 38 (1998) 1843.
[37] X. Wang, E. Brunger, G. Gottstein, Mater. Sci. Eng. A 290 (2000) 180.